Density Functional Study of the Conformations and Vibrations of 1,2-Dimethoxyethane

Hiroshi Yoshida and Hiroatsu Matsuura*

Department of Chemistry, Faculty of Science, Hiroshima University, Kagamiyama,
Higashi-Hiroshima 739-8526, Japan

Received: November 4, 1997; In Final Form: February 6, 1998

The conformations and vibrations of 1,2-dimethoxyethane (DME) have been studied by density functional theory (DFT) in comparison with the molecular orbital (MO) methods. The calculations using the 6-31G* basis set were performed by five DFT methods (BVWN, BP86, BLYP, B3PW91, and B3LYP) and two MO methods (HF and MP2). The energies of conformers were better predicted by the DFT methods using the B3 exchange functional than other methods. The vibrational wavenumbers calculated by the DFT and MO methods explained, after correcting with uniform scaling, the observed Raman and infrared spectra of the normal and perdeuterated species of DME. It was confirmed that the conformer of DME present in the solid state is TGT, and the conformers in the liquid state are TGT, TTT, TGG′, and TTG. The present calculations further indicated that the TGG and GGG conformers are also present in the liquid state. The distributions of the ratio of the unscaled calculated wavenumber to the experimental wavenumber are narrower with the B3PW91 and B3LYP methods than with other methods, indicating that these two methods, when making appropriate uniform scaling corrections, give wavenumbers in excellent agreement with the experimental wavenumbers. In conclusion, the performance of the B3PW91 and B3LYP methods is the best among the DFT and MO methods used in this work in reproducing the experimental results of the energies, molecular geometries, and vibrational wavenumbers for DME.

Introduction

Vibrational analysis has played for a long time an important role in the determination of the molecular structures and intramolecular potentials for a variety of compounds. Since the GF matrix method was proposed by Wilson,[1] a great number of vibrational analyses have been performed by using empirical molecular force fields[2−4] and have contributed significantly to the development of structural chemistry. As a result of these studies, a huge number of force constants have been accumulated, and those for fundamental organic compounds have been compiled as a database.[5,6] Although the classical method of vibrational analysis using empirical force fields has been successful in many cases, several problems have been encountered in other cases. Some of the relevant problems are that (1) the off-diagonal force constants are normally difficult to determine statistically from available experimental data, (2) the force constants for conjugated systems and hydrogen-bonding systems are difficult to estimate, and (3) the force constants in electronic excited states are not easy to determine empirically.

Since the pioneering work in the 1970s,[7−9] ab initio molecular orbital (MO) calculations have been rapidly developed and the accuracy of ab initio force constants derived therefrom has been greatly improved. Vibrational analysis by the quantum chemical method has actually been a breakthrough of the difficulties encountered in the classical method. The ab initio vibrational wavenumbers[10] were, however, overestimated by about 10% in the Hartree−Fock (HF) calculations on account of the neglect of electron correlation and anharmonicity effects. The scaled quantum mechanical method proposed by Pulay et al.[12] has then become one of the most successful techniques in vibrational analysis.[13] To get more accurate predictions of vibrational spectra, more time-consuming methods of calculations including electron correlation, such as the second-order Møller−Plesset perturbation theory (MP2), have been put forward. These methods are, however, applicable practically only to relatively small molecules because of the CPU time required. The recent introduction of density functional theory (DFT),[14] which includes electron correlation in an alternative way, has afforded opportunities of performing vibrational analysis of moderately large molecules.[15] Among various types of density functionals available, those which use Becke's three-parameter exchange functional[16] are the most promising in providing excellent results of molecular geometries and vibrational wavenumbers.[17−20]

In the present work, we have examined the performance of the DFT methods, in comparison with that of the MO methods, in conformational and vibrational analyses of 1,2-dimethoxyethane (DME). This molecule was selected for the present investigation for the following reasons. (1) There have been a large number of theoretical conformational studies on this molecule, but the energies of conformers are considerably different depending on the method of calculations.[21−25] (2) Experimental evidence of the conformational stabilities of an isolated DME molecule has been a controversial issue,[22,26−29] although there is a general agreement on the conformational preference in the solid and liquid states. (3) The experimental vibrational spectra have been well characterized for the normal species ($CH_3OCH_2CH_2OCH_3$) and the perdeuterated species ($CD_3OCD_2CD_2OCD_3$), and the observed bands have been accurately assigned.[22,26,30] The conformation of this molecule will be denoted by specifying the conformational state of the three consecutive bonds CO−C−C−OC with T for trans, G for gauche, and G′ for another gauche with the opposite direction of rotation. Before describing the details of the present work, we briefly review the previous theoretical studies of DME.

The previous studies have been done in most cases to understand fundamental properties of the conformation of poly-

S1089-5639(98)00076-0 CCC: $15.00

(oxyethylene) $(-OCH_2CH_2-)_m$,[31] because DME is the simplest model compound for this polymer, corresponding to its monomeric unit. Andersson and Karlström have calculated the energy of the TGT conformer to be 0.9 kcal mol^{-1} relative to that of the TTT conformer by the HF method using a basis set of double zeta and polarization quality.[32] Barzaghi et al. have shown by performing the MP2/6-31G*//HF/6-31G* calculations including electron correlation and by extrapolating to the MP4(SDQ)/6-31G** level that the TGT conformer has an energy higher than the TTT conformer by 0.61 kcal mol^{-1}.[21] Murcko and DiPaola have reported that the energy of the TGT conformer is 0.38 kcal mol^{-1} higher than that of the TTT conformer when calculated at the MP4(SDTQ)/6-31+G*//HF/6-31G* level, while it amounts to 1.41 kcal mol^{-1} at the HF level using the same basis set.[23]

We have previously calculated the energies of nine conformers of DME at the HF level and have shown that the TTT conformer is the most stable and the TGG′ conformer follows this.[22] Tsuzuki et al. have conducted more accurate calculations on nine conformers at the MP3/6-311+G*//HF/6-311+G* level.[24] The energy of the TGG′ conformer was calculated to be higher than that of the most stable TTT conformer by only 0.53 kcal mol^{-1}, and the high stability of the TGG′ conformer was ascribed to a nonbonded attractive interaction between the methyl hydrogen atom and the oxygen atom (1,5-CH···O interaction). The possible existence of this interaction had been suggested by Astrup in his electron diffraction study to explain the dominant presence of the TGG′ conformer in the gas phase.[27] The importance of the 1,5-CH···O interaction in the stabilization of the TGG′ conformer was experimentally shown by matrix-isolation infrared spectroscopy.[22] Tsuzuki et al. also calculated the energies of the TTT and TGT conformers with different basis sets and methods.[24] The most improved calculations at the MP4(SDQ)/6-311++G*//HF/6-311+G* level gave 0.39 kcal mol^{-1} for an energy of the TGT conformer relative to that of the TTT conformer, while the calculations at the MP3/6-311+G*//HF/6-311+G* and MP3/6-311++G*//HF/6-311+G* levels gave 0.51 and 0.47 kcal mol^{-1}, respectively, for the corresponding energy.

Jaffe et al. have subsequently calculated the energies of 10 possible conformers of DME at the MP2 level using the D95+(2df,p) basis set and have shown that the energy of the TGG′ conformer lies only 0.23 kcal mol^{-1} above the energy of the TTT conformer apparently due to the 1,5-CH···O interaction and that the energy of the TGT conformer is higher than that of the TTT conformer by 0.14 kcal mol^{-1}.[25] The MP2 calculations using larger basis sets D95+(+)(2df,p) and 6-311+G(2df,p) yielded an energy of the TGT conformer 0.14 and 0.22 kcal mol^{-1}, respectively, relative to that of the TTT conformer.[25] Gas-phase infrared spectroscopy has recently shown that the energy of the TGG′ conformer is 0.31 kcal mol^{-1} higher than that of the TTT conformer.[29] The previous ab initio MO calculations have indicated that the inclusion of electron correlation is necessary to reproduce the experimental energy of the TGG′ conformer, which is stabilized by the 1,5-CH···O interaction. In the present study, we have examined the conformational stabilities of DME by performing various DFT calculations which include electron correlation.

The vibrational wavenumbers of DME have been calculated by Murcko and DiPaola at the HF/6-31G* level for the TTT, TGT, and TTG conformers[23] and by Jaffe et al. at the HF/D95** level for the TTT, TGT, and TGG′ conformers.[25] The wavenumbers calculated by the two methods for the TGT conformer agree well with the experimental values, if the calculated wavenumbers are scaled by a factor of 0.9. In this work, we have studied the performance of the DFT methods in reproducing the experimental wavenumbers for the normal and perdeuterated species of DME.

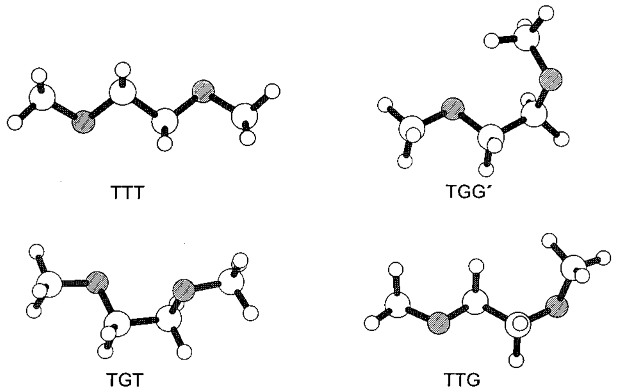

Figure 1. Structures of four low-energy conformers of 1,2-dimethoxyethane.

Calculations

In the present calculations on DME, we employed the ab initio MO methods of HF and MP2 and the DFT methods using the Becke (B) exchange functional[33] and Becke's three-parameter (B3) exchange functional.[16] The B exchange functional was combined with the Vosko−Wilk−Nussair functional[34] (BVWN), the Perdew correlation functional[35] (BP86), and the Lee−Yang−Parr correlation functional[36] (BLYP), and the B3 exchange functional was combined with the Perdew−Wang correlation functional[37−39] (B3PW91) and the Lee−Yang−Parr correlation functional (B3LYP). The calculations by these methods were performed by using the 6-31G* basis set. The energies, molecular geometries, and harmonic vibrational wavenumbers for four low-energy conformers, TTT, TGG′, TGT, and TTG, whose structures are depicted in Figure 1, were calculated by all seven methods, and those for the TGG and GGG conformers were calculated by the MP2 and B3LYP methods.

The computation was carried out with the GAUSSIAN 94 program[40] by using the default parameters. The normal coordinate calculations were performed by using uniform wavenumber scale factors for the respective force fields: 0.89 for HF, 0.95 for MP2, 0.98 for BVWN, 1.00 for BP86, 1.00 for BLYP, 0.97 for B3PW91, and 0.97 for B3LYP. These scale factors were chosen so that the calculated wavenumbers for the TGT conformer of DME and the most stable conformers of related compounds, 2-methoxyethanol and 2-(methylthio)-ethanol,[20] fit best with the experimental wavenumbers. These scale factors are actually close to those derived from a large number of experimental wavenumbers for fundamental polyatomic molecules.[19] The force constants in terms of the group symmetry coordinates[4] and the potential-energy distributions for normal vibrations based on these coordinates were obtained from the results of the MO and DFT calculations by using a modified program of NCTB.[41,42]

Results and Discussion

Energies. The energies of the TTT, TGG′, TGT, and TTG conformers calculated by various MO and DFT methods are given in Table 1, where the zero-point energies calculated by the MP2 and B3LYP methods are also given. These conformers have been confirmed to exist in the liquid state[26,30] and in an argon matrix.[22] The HF calculations predicted the energies of the TGG′ and TGT conformers to be higher than the energy of

TABLE 1: Relative Energies (kcal mol^{-1}) of Four Low-Energy Conformers of 1,2-Dimethoxyethane

conformer[a]	calculated[b]								experimental[d]
	HF	MP2	BVWN	BP86	BLYP	B3PW91	B3LYP	MP3[c]	
TTT	0.0	0.0 (0.0)	0.0	0.0	0.0	0.0	0.0 (0.0)	0.0	0.0
TGG′	1.648	0.094 (0.066)	0.468	0.014	−0.029	0.497	0.308 (0.149)	0.529	0.31
TGT	1.404	0.570 (−0.048)	0.451	0.162	0.207	0.517	0.506 (−0.020)	0.508	
TTG	1.822	1.469 (0.022)	1.286	1.181	1.267	1.383	1.398 (0.103)	1.645	

[a] Energies, in kcal mol^{-1}, of other conformers calculated at the MP3/6-311+G*//HF/6-311+G* level are 1.971 for GGG, 2.242 for TGG, 2.298 for GGG′, 3.344 for GTG′, and 3.466 for GTG.[24] [b] The 6-31G* basis set was used in the calculations except for the MP3 method. The zero-point energies, in kcal mol^{-1}, calculated by the MP2 and B3LYP methods are given in parentheses. [c] Calculated at the MP3/6-311+G*//HF/6-311+G* level.[24] [d] Relative enthalpies determined by infrared spectroscopy in the gas phase.[29]

TABLE 2: Geometries of the TGT Conformer of 1,2-Dimethoxyethane

structural parameter[a]	calculated[b]							experimetal[c]	
	HF	MP2	BVWN	BP86	BLYP	B3PW91	B3LYP	crystal[d]	gas[e]
				Bond Lengths/Å					
C_1-O_2	1.3912	1.4167	1.4296	1.4185	1.4262	1.4040	1.4099	1.4196(14)	1.410(3)
O_2-C_3	1.3925	1.4158	1.4330	1.4213	1.4292	1.4064	1.4123	1.4188(12)	1.410(3)
C_3-C_4	1.5107	1.5079	1.5302	1.5207	1.5266	1.5119	1.5158	1.496(2)	1.504[f]
				Valence Angles/deg					
$C_1-O_2-C_3$	114.17	111.38	112.80	111.72	112.31	112.38	112.70	111.26(8)	110.7(1.4)
$O_2-C_3-C_4$	109.31	108.38	109.37	109.26	109.14	109.37	109.25	109.76(8)	113.2(1.6)
				Torsion Angles/deg					
$C_1-O_2-C_3-C_4$	−175.52	−176.27	−176.71	−176.98	−176.97	−176.22	−176.35	175.95(7)	152.4(6.0)
$O_2-C_3-C_4-O_5$	71.84	71.35	73.58	72.68	72.85	72.43	72.47	69.10(15)	61.9(7.8)

[a] Atoms are numbered as $C_1-O_2-C_3-C_4-O_5-C_6$. [b] The 6-31G* basis set was used in the calculation. [c] Error given in parentheses applies to the last significant digit(s). [d] X-ray diffraction.[43] [e] Electron diffraction.[27] [f] Assumed.

the TTT conformer by more than 1.4 kcal mol^{-1}. This tendency of large energy difference between the TGT and TTT conformers, when calculated by the HF method without including electron correlation, has been shown in previous studies.[22−25] The MP2 and DFT calculations including electron correlation, on the other hand, gave the energies of the TGG′ and TGT conformers to be less than 0.6 kcal mol^{-1} above the energy of the TTT conformer. In contrast with the great stabilization of the TGG′ and TGT conformers by electron correlation effects, the TTG conformer is practically not stabilized in the MP2 and DFT calculations. It is clear from these results that electron correlation effects significantly decrease the energy of the gauche conformation around the OC−CO bond, but does not affect the energy of the trans conformation.

Gas-phase infrared spectroscopy gave an enthalpy difference 0.31 ± 0.04 kcal mol^{-1} between the TGG′ and TTT conformers.[29] The energies calculated by the BVWN, B3PW91, and B3LYP methods are in better agreement with this experimental observation than those by other methods when the zero-point energies are taken into consideration. Further stabilization of the TGG′ conformer resulted if the MP2, BP86, and BLYP methods were used for calculations, leading to the energy difference between the TGG′ and TTT conformers to be smaller than the experimental result. These methods probably overestimate the effect of the 1,5-CH···O interaction in the TGG′ conformer. The energy difference between the TGT and TGG′ conformers was predicted to be less than 0.2 kcal mol^{-1} in the present DFT calculations. No experimental observations are available, however, to evaluate this theoretical prediction.

It may be concluded from the present results that the energies of the conformers of DME are better predicted by the DFT methods using the B3 exchange functional than other DFT and MO methods. The results of the DFT calculations by the B3LYP and B3PW91 methods are close in general to those of the high-level MO calculations by the MP3 and MP4 methods.[23,24] To evaluate the performance of the theoretical methods in the prediction of the conformational energies of DME, further experimental studies of the conformational stabilities in the gas phase are necessary.

In a previous gas-phase NMR study of DME, Inomata and Abe have performed a rotational isomeric state analysis and obtained −0.4 kcal mol^{-1} for the energy difference between the TGT and TTT conformers, the former being more stable.[28] This energy difference is, however, not consistent with the results of ab initio MO and DFT calculations so far reported.

Molecular Geometries. The bond lengths, valence angles, and torsion angles of the TGT conformer of DME optimized by various methods of calculations are given in Table 2. The geometries of the conformers of DME have been calculated previously,[23−25] but no comparative discussions of the results by different calculation methods have been made. The calculated results may be compared with the experimental molecular geometries in crystals determined by X-ray diffraction;[43] the molecule in crystals has been shown to assume the TGT conformation.

The present results indicate that the bond lengths calculated by the HF method are shorter, while those by the BVWN, BP86, and BLYP methods are longer, than the corresponding bond lengths calculated by other methods. This tendency of the changes in bond length by the method of calculations has also been observed in the previous calculations on analogous molecules 2-methoxyethanol and 2-(methylthio)ethanol.[20] The valence angles and torsion angles are, on the other hand, not significantly different with the calculation method used.

A comparison of the calculated results with the X-ray diffraction observations[43] (Table 2) indicates that the geometries of the TGT conformer in crystals are well explained by the calculations on a free molecule except for the CO−CC torsion angle. It is noticed that the CO−CC torsion angle in crystals differs by 7−8° from the angle theoretically calculated, apparently due to intermolecular interactions. The X-ray diffraction study has in fact shown the possibility of intermolecular

TABLE 3: Vibrational Wavenumbers[a] (cm^{-1}) and Assignments for the TGT Conformer of the Normal Species of 1,2-Dimethoxyethane, $CH_3OCH_2CH_2OCH_3$

	calculated[c]								experimental[e]			
sym[b]	HF	MP2	BVWN	BP86	BLYP	B3PW91	B3LYP	emp[d]	gas	liquid	solid	assignment[f]
A	1489	1501	1503	1500	1510	1500	1503	1491		1490[g]	1492	CH_2 scis (42), CH_3 asym def (28), CH_3 sym def (19)
B	1489	1502	1503	1500	1509	1500	1503	1491		1490[g]	1492	CH_2 scis (44), CH_3 asym def (30), CH_3 sym def (18)
A	1473	1486	1484	1477	1488	1479	1483	1479		1470	1472	CH_3 asym def (60), CH_2 scis (38)
B	1471	1484	1482	1475	1486	1477	1481	1466		1470	1472	CH_3 asym def (60), CH_2 scis (38)
A	1465	1475	1469	1462	1472	1467	1469	1466	1460	1459[g]	1461	CH_3 asym def (97)
B	1465	1474	1469	1462	1472	1466	1469	1463	1460	1459[g]	1461	CH_3 asym def (97)
A	1459	1453	1454	1448	1459	1454	1458	1461		1450	1453	CH_3 sym def (72), CH_2 scis (18)
B	1453	1450	1454	1447	1458	1452	1456	1459		1450	1453	CH_3 sym def (80), CH_2 scis (17)
A	1426	1410	1401	1403	1410	1414	1416	1409	1396[g]	1410	1417	CH_2 wag (74), C−C str (18), CH_3 sym def (15)
B	1381	1363	1370	1361	1374	1369	1375	1369	1365[g]	1365	1370	CH_2 wag (93)
A	1283	1272	1269	1274	1277	1284	1282	1287	1285	1285	1288	CH_2 twist (78)
B	1247	1231	1225	1231	1233	1242	1240	1249	1255	1250	1244	CH_2 twist (71), CH_3 rock (11)
B	1213	1195	1185	1193	1195	1205	1203	1208	1204[g]	1208	1202	CH_3 rock (56), C−O str (16), CH_2 twist (10)
A	1215	1193	1184	1190	1193	1203	1200	1208	1204[g]	1208	1202	CH_3 rock (59), C−O str (16)
A	1168	1159	1146	1154	1157	1172	1162	1163	1160	1155	1171	CH_3 rock (63), CH_3−O str (13)
B	1154	1147	1143	1149	1153	1155	1155	1152	1160	1155	1171	CH_3 rock (89)
A	1154	1145	1074	1143	1118	1156	1149	1143	1160	1155	1171	CH_3−O str (39), CH_3 rock (29), C−O str (21)
B	1141	1122	1059	1120	1094	1147	1128	1096	1125	1131	1131	CH_3−O str (67), C−O str (29)
A	1094	1098	1090	1093	1094	1098	1098	1089	1095[g]	1092	1102	CH_2 rock (53), CH_3 rock (20)
B	1038	1028	1007	1031	1024	1042	1035	1041	1035	1032	1036	CH_2 rock (33), CH_3−O str (21), C−O str (16)
A	1017	1021	973	1019	1000	1033	1019	1028	1020	1022	1026	CH_3−O str (40), C−C str (36)
B	859	854	824	852	843	863	856	852	848	848	857	CH_2 rock (42), C−O str (40), CH_3−O str (16)
A	846	853	817	849	838	858	850	860	848	848	857	C−O str (38), CH_2 rock (20), C−C str (18)
B	550	560	548	559	558	560	559	567	565	568	585	CCO def (36), COC bend (29), CH_2 rock (14)
A	348	356	346	355	354	354	354	362	365	365	370	COC bend (47), CCO def (19), C−C str (11)
B	300	308	300	305	305	305	306	327		326	326	COC bend (65), CCO def (39)
A	262	273	269	277	277	273	273	283		280	267	CCO def (39), COC bend (34), C−C tor (18)
A	220	232	226	235	232	232	230	216			205	CH_3−O tor (73), COC bend (19)
B	209	225	222	233	231	228	225	211			205	CH_3−O tor (98)
A	119	121	117	119	118	120	119	123				C−C tor (80), CH_3−O tor (13)
B	75	78	74	78	77	78	78	95				C−O tor (93)
A	71	75	69	73	73	73	73	98				C−O tor (87), CCO def (19)

[a] Wavenumbers higher than 1550 cm^{-1} are not given in this table. [b] Symmetry species of the normal vibrations for a point group C_2 molecule. [c] The 6-31G* basis set was used in the calculation. The calculated wavenumbers have been scaled by 0.89 for HF, 0.95 for MP2, 0.98 for BVWN, 1.00 for BP86, 1.00 for BLYP, 0.97 for B3PW91, and 0.97 for B3LYP. [d] Calculated by using empirical force constants.[30] [e] Raman spectroscopy[26] unless otherwise indicated. [f] Assignment based on the potential-energy distributions, given in parentheses in %, calculated by the B3LYP method. Key: sym, symmetric; asym, asymmetric; scis, scissor; def, deformation; str, stretch; tor, torsion. C−O implies CH_2−O. [g] Infrared spectroscopy.[26]

interactions between the methyl group and the oxygen atom and between the methylene group and the oxygen atom.[43] These intermolecular CH···O interactions may be responsible for the stabilization of the TGT conformer in crystals. The distortion of the CO−CC torsion angle from the angle for a free molecule most probably results in favorable intermolecular interactions between the methyl group and the oxygen atom.

The molecular geometries in the gas phase have been determined from an electron diffraction experiment.[27] Because of the difficulties in the analysis due to the coexistence of several conformers, the values obtained for structural parameters are not precise enough to be compared with the theoretical values.

Vibrational Analysis. The Raman and infrared spectra of the normal species of DME, $CH_3OCH_2CH_2OCH_3$, have been studied extensively[26,44−47] in relation to the conformational elucidation of poly(oxyethylene).[48−50] The assignments of the Raman and infrared bands have been thoroughly examined by performing detailed spectral measurements[26] and systematic normal coordinate analysis.[5,30,51] Since the molecular conformation of DME in the solid state has been established to be TGT,[26,43] the vibrational wavenumbers for this conformer are unambiguously identified in the spectra. The Raman spectra of the perdeuterated species of DME (1,2-dimethoxyethane-d_{10}), $CD_3OCD_2CD_2OCD_3$, have been measured and the observed bands have been assigned on the basis of normal coordinate analysis.[30] The use of deuterated compounds in vibrational analysis used to be important in making correct band assignments and in deriving reliable empirical force constants.[2] The vibrational data of these compounds are still important for evaluating the performance of ab initio theoretical calculations.

(a) TGT Conformer. Tables 3 and 4 give the vibrational wavenumbers for the TGT conformer of the normal and perdeuterated species, respectively, of DME calculated by various MO and DFT methods and those calculated by using empirical force constants. The wavenumbers have been scaled by 0.89 for HF, 0.95 for MP2, 0.98 for BVWN, 1.00 for BP86, 1.00 for BLYP, 0.97 for B3PW91, and 0.97 for B3LYP. In these tables, the experimental wavenumbers in the solid state as well as the corresponding wavenumbers in the gaseous and liquid states are also given. The band assignments are essentially the same as those previously reported.[5,26,30] It should be mentioned that the wavenumbers for the same normal vibrations are slightly different between the Raman and infrared spectra in most cases. In Table 3, the wavenumbers in the Raman spectra were preferentially adopted as the experimental wavenumbers for the normal species.

To examine the performance of the respective theoretical methods in reproducing the experimental wavenumbers for the TGT conformer of the two isotopic species, the histogram of the ratio of the unscaled calculated wavenumber to the

TABLE 4: Vibrational Wavenumbers[a] (cm^{-1}) and Assignments for the TGT Conformer of the Perdeuterated Species of 1,2-Dimethoxyethane, $CD_3OCD_2CD_2OCD_3$

	calculated[c]								experimental[e]		
sym[b]	HF	MP2	BVWN	BP86	BLYP	B3PW91	B3LYP	emp[d]	liquid	solid	assignment[f]
A	1282	1277	1220	1257	1245	1275	1265	1260	1265	1275	C−C str (54), CD_2 wag (48), C−O str (19)
B	1187	1167	1145	1159	1157	1179	1168	1146	1146	1150	C−O str (52), CD_2 wag (41)
A	1177	1158	1110	1151	1133	1177	1162	1140	1146	1150	CD_3−O str (58), CD_3 sym def (39), C−O str (25)
B	1164	1147	1097	1139	1119	1163	1151	1107	1128	1129	CD_3−O str (67), CD_3 sym def (56)
A	1148	1143	1131	1139	1140	1147	1144	1117	1128	1129	CD_2 scis (40), CD_3 sym def (31), C−O str (19)
B	1094	1093	1091	1087	1097	1090	1095	1088	1091	1098	CD_2 scis (68), CD_2 wag (16)
A	1068	1079	1076	1071	1079	1071	1075	1069	1073	1074	CD_3 asym def (99)
B	1068	1079	1075	1071	1078	1071	1074	1066	1068	1069	CD_3 asym def (98)
A	1060	1069	1065	1058	1066	1061	1063	1049	1057	1054	CD_3 asym def (100)
B	1060	1069	1065	1058	1066	1060	1063	1049	1057	1054	CD_3 asym def (100)
A	1052	1052	1040	1054	1055	1058	1058	1042	1057	1054	CD_2 scis (38), CD_3 sym def (20), C−O str (11)
B	1049	1041	1035	1048	1049	1053	1053	1036	1057	1054	CD_2 wag (29), CD_3 rock (18), CD_3 sym def (17)
A	1009	1000	983	1004	997	1012	1007	992	1008	1009	CD_3−O str (23), CD_3 rock (14), CD_3 sym def (14)
B	1008	999	979	1004	999	1012	1007	988	1008	1009	CD_3−O str (29), CD_3 sym def (17), CD_3 rock (13)
A	933	928	923	932	933	937	936	955	948	938	CD_3 rock (33), CD_2 twist (26), CD_2 rock (26)
B	933	926	923	932	933	937	936	954	948	938	CD_2 twist (38), CD_3 rock (35), CD_2 rock (19)
A	910	912	900	908	909	913	912	909	927	927	CD_2 twist (31), CD_3 rock (25), C−C str (10)
A	875	867	864	871	871	876	875	879	882	885	CD_3 rock (64), CD_2 twist (15)
B	874	866	863	870	871	875	874	873	882	885	CD_3 rock (62), CD_2 twist (27)
B	848	843	839	850	849	854	852	853	854	859	CD_3 rock (56), C−O str (9), CCO def (8)
A	840	838	829	845	841	850	846	853	854	855	CD_3 rock (34), CD_2 wag (20), C−O str (15)
B	719	717	703	718	714	724	720	702	717	728	CD_2 rock (35), CD_2 twist (26), C−O str (23)
A	706	715	698	712	710	716	713	718	717	728	CD_2 rock (23), CD_2 wag (21), C−C str (21)
B	470	477	468	473	474	474	475	493	482	492	CCO def (28), COC bend (26), CD_2 rock (25)
A	310	317	308	315	315	315	315	327	329	331	COC bend (50), CCO def (17), C−C str (10)
B	258	265	258	261	262	261	262	289		281	COC bend (63), CCO def (38)
A	219	227	223	227	227	226	226	236	239		CCO def (54), COC bend (31), C−C tor (13)
A	181	188	184	191	189	189	187	178		206	CD_3−O tor (71), C−C tor (19)
B	159	170	167	175	174	171	170	161		175	CD_3−O tor (99)
A	96	99	95	98	98	98	97	98			C−C tor (71), CD_3−O tor (28)
B	65	67	64	68	68	68	68	88			C−O tor (92)
A	62	66	62	65	65	65	65	81			C−O tor (88), CCO def (18)

[a] Wavenumbers higher than 1300 cm^{-1} are not given in this table. [b] Symmetry species of the normal vibrations for a point group C_2 molecule. [c] The 6-31G* basis set was used in the calculation. The calculated wavenumbers have been scaled by 0.89 for HF, 0.95 for MP2, 0.98 for BVWN, 1.00 for BP86, 1.00 for BLYP, 0.97 for B3PW91, and 0.97 for B3LYP. [d] Calculated by using empirical force constants.[30] [e] Raman spectroscopy.[30] [f] Assignment based on the potential-energy distributions, given in parentheses in %, calculated by the B3LYP method. Key: sym, symmetric; asym, asymmetric; scis, scissor; def, deformation; str, stretch; tor, torsion. C−O implies CD_2−O.

experimental wavenumber, ν_{calc}/ν_{exp}, is drawn in Figure 2, where the experimental wavenumbers are those observed in the Raman spectra in the solid state (Tables 3 and 4). The histogram indicates that the unscaled wavenumbers calculated by the HF

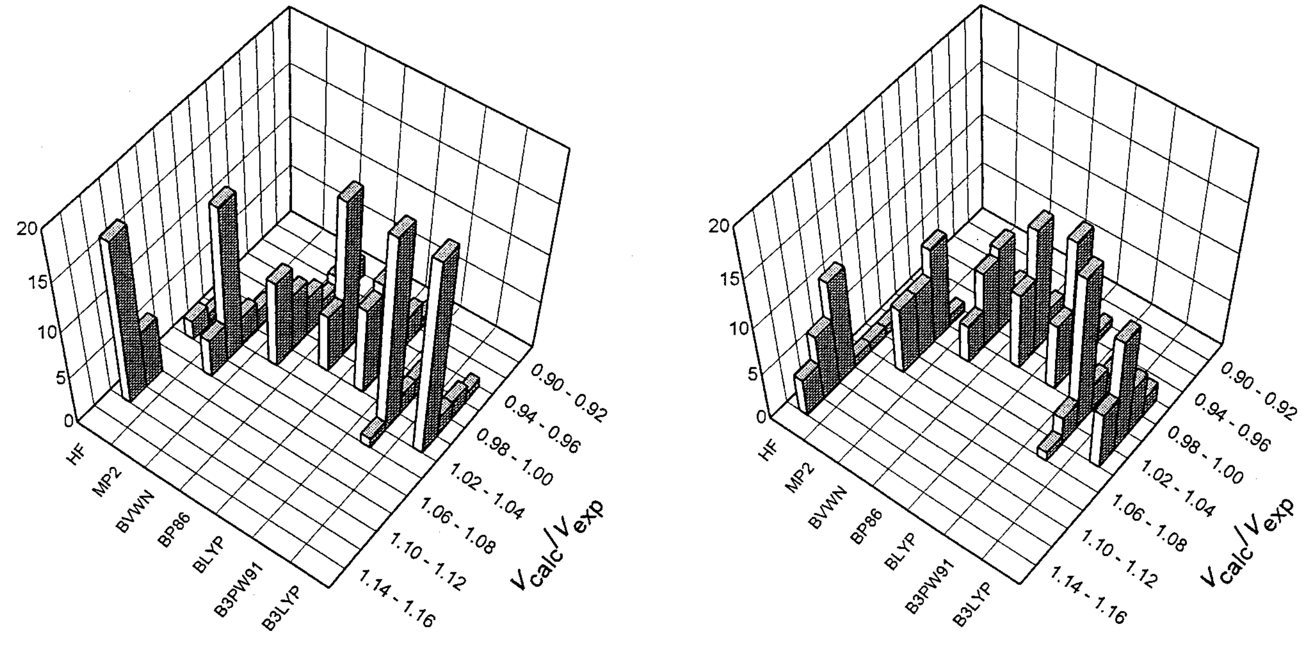

(a) (b)

Figure 2. Histogram of the ratio of the unscaled calculated wavenumber to the experimental wavenumber, ν_{calc}/ν_{exp}, for the TGT conformer of (a) the normal species and (b) the perdeuterated species of 1,2-dimethoxyethane. The experimental wavenumbers are those observed in the Raman spectra in the solid state above 300 cm^{-1}.

TABLE 5: Vibrational Wavenumbers[a] (cm^{-1}) for the TTT, TGG′, and TTG Conformers of the Normal Species of 1,2-Dimethoxyethane, $CH_3OCH_2CH_2OCH_3$

	TTT				TGG′				TTG			
	calculated[c]				calculated[c]				calculated[c]			
sym[b]	MP2	B3LYP	emp[d]	exptl[e]	MP2	B3LYP	emp[d, f]	exptl[e]	MP2	B3LYP	emp[d]	exptl[e]
B_u	1518	1520	1491	1490[g]	1503	1504	1491	1490[g]	1514	1515	1491	1490[g]
A_g	1512	1512	1491		1496	1497	1491	1490[g]	1495	1494	1491	1490[g]
B_u	1492	1489	1480	1479[g]	1484	1482	1476	1470	1492	1489	1479	1470
A_g	1491	1488	1465	1470	1474	1471	1467	1459[g]	1487	1484	1466	1470
B_g	1475	1468	1466	1470	1473	1469	1466	1459[g]	1478	1474	1466	1459[g]
A_u	1474	1468	1466	1459[g]	1468	1467	1463	1459[g]	1475	1470	1463	1459[g]
A_g	1457	1463	1460	1450	1450	1456	1462	1450	1454	1460	1461	1450
B_u	1450	1456	1461	1451[g]	1447	1450	1458	1450	1451	1456	1457	1450
A_g	1416	1421	1411	1410	1393	1400	1403	1395	1403	1412	1407	1410
B_u	1321	1338	1345	1338[g]	1361	1376	1368	1365	1314	1334	1343	1338[g]
B_g	1265	1270	1269	1270	1299	1312	1303	1301	1284	1294	1297	1301
A_g	1207	1213	1209	1208	1236	1249	1262	1250	1237	1246	1269	1250
A_u	1203	1212	1269	1210[g]	1202	1209	1212	1208	1194	1201	1210	1208
B_u	1187	1194	1205	1195[g]	1184	1191	1205	1195	1191	1199	1205	1195
B_g	1165	1171	1194		1152	1159	1163	1155	1166	1171	1194	
A_u	1146	1153	1154	1160[g]	1150	1156	1154	1155	1146	1152	1159	1155
A_g	1137	1140	1127	1138	1143	1143	1131	1138	1139	1144	1148	1138
B_u	1134	1141	1114	1130[g]	1120	1124	1095	1122[g]	1133	1138	1123	1131
B_g	1128	1132	1138	1131	1088	1089	1088	1092	1094	1098	1069	1108
A_g	1067	1056	1056	1063	1021	1022	1032	1022	1055	1039	1059	1053
A_g	989	995	996	996	974	976	986	985	968	973	971	970
B_u	938	946	929	938[g]	866	868	861	868[g]	921	927	928	923
A_u	822	821	825	823[g]	817	815	853	822	798	802	822	822
B_u	492	492	522	513[g]	528	527	538	540	465	466	485	483
A_g	385	386	402	396	402	402	399	420	430	429	436	440
A_g	324	322	338		353	350	374	352	359	358	375	365
A_u	239	235	233		268	264	287	280	231	231	241	
B_g	222	219	208		231	231	216		224	225	217	
B_u	143	140	150		203	191	193		158	157	169	
B_g	121	121	153		119	124	113		112	119	140	
A_u	103	99	131		87	90	95		84	82	107	
A_u	69	68	80		61	75	87		62	70	89	

[a] Wavenumbers higher than 1550 cm^{-1} are not given in this table. [b] Symmetry species of the normal vibrations for a point group C_{2h} molecule. [c] The 6-31G* basis set was used in the calculation. The calculated wavenumbers have been scaled by 0.95 for MP2 and 0.97 for B3LYP. [d] Calculated by using empirical force constants.[30] [e] Raman spectroscopy in the liquid state[26] unless otherwise indicated. [f] Calculated in the present work. [g] Infrared spectroscopy in the liquid state.[26]

and MP2 methods are larger than the experimental wavenumbers by about 10% and 5%, respectively, on average. The DFT calculations gave a better agreement between the theoretical and experimental wavenumbers than the MO calculations; the DFT methods overestimated most of the wavenumbers by only 3% or less.

The histogram in Figure 2 shows that the distributions of the ν_{calc}/ν_{exp} ratio are narrower with the B3PW91 and B3LYP methods than with other methods, indicating that these two methods, when making appropriate uniform scaling corrections, give wavenumbers in excellent agreement with the experimental wavenumbers. Although the BVWN, BP86, and BLYP methods give rather large distributions of the ν_{calc}/ν_{exp} ratio, the calculated wavenumbers by these methods agree on average with the experimental wavenumbers without making empirical corrections to the calculated values. Summarizing the performance of the theoretical methods employed in this work, we conclude that the DFT methods using the B3 exchange functional, namely, the B3PW91 and B3LYP methods, best reproduced the experimental wavenumbers.

(b) TTT, TGG′, and TTG Conformers. Tables 5 and 6 give the vibrational wavenumbers for the TTT, TGG′, and TTG conformers of the normal and perdeuterated species, respectively, calculated by the MP2 and B3LYP methods and those calculated by using empirical force constants. The wavenumbers have been scaled by the same factors as applied to the TGT conformer. The experimental wavenumbers by Raman and infrared spectroscopy are also given in these tables. The previous detailed vibrational analyses of the two isotopic species of DME have clarified the vibrational assignments of the observed bands and have shown that the TGT, TTT, TGG, and TTG conformers exist in the liquid and gaseous states.[26,30] The temperature dependence of the Raman spectra indicated that the stabilities of the conformers in the liquid state are in the order TGT > TTT > TGG > TTG.[26] The conformer TGG considered in the previous analyses should now be replaced by TGG′ in the light of the recent molecular dynamics simulations[52] showing that the populations of the TGG′ and TGG conformers are 34% and 4%, respectively, in the gas phase and are 17% and 8% in the liquid phase. The wavenumbers for the TGG conformer calculated by the MP2 and B3LYP methods (the results are not given here) as well as those calculated by using empirical force constants are similar to those for the TGG′ conformer. The reasoning mentioned above justifies the presence of the TGG′ conformer in preference to the TGG conformer in the liquid and gaseous states.

The observed Raman and infrared bands of the normal and perdeuterated species in the liquid state are assigned to the TGT, TTT, TGG′, and TTG conformers, as shown in Tables 3−6, on the basis of the present calculations. The assignments of the bands to the TTT, TGG′, and TTG conformers are essentially the same as the previous ones,[26,30] although several changes of the assignments were made owing to the present more sophisticated calculations.

TABLE 6: Vibrational Wavenumbers[a] (cm^{-1}) for the TTT, TGG′, and TTG Conformers of the Perdeuterated Species of 1,2-Dimethoxyethane, $CD_3OCD_2CD_2OCD_3$

	TTT				TGG′				TTG			
	calculated[c]				calculated[c]				calculated[c]			
sym[b]	MP2	B3LYP	emp[d]	exptl[e]	MP2	B3LYP	emp[d, f]	exptl[e]	MP2	B3LYP	emp[d]	exptl[e]
A_g	1277	1266	1261	1265	1245	1231	1237	1232	1243	1231	1239	1232
B_u	1161	1166	1156		1158	1162	1147	1146	1158	1158	1146	1146
A_g	1160	1161	1129	1146	1149	1152	1136	1141	1151	1157	1139	1141
A_g	1151	1156	1102	1141	1144	1144	1117	1128	1144	1143	1116	1128
B_u	1137	1143	1120		1133	1133	1105	1128	1131	1138	1104	1128
B_u	1105	1110	1094		1081	1080	1082	1091	1096	1096	1080	1091
A_g	1080	1075	1067	1073	1081	1078	1069	1073	1080	1076	1066	1073
B_u	1080	1075	1067		1078	1074	1066	1068	1079	1075	1065	1068
B_g	1069	1063	1049	1057	1069	1064	1060	1057	1071	1066	1057	1057
A_u	1069	1063	1049		1067	1063	1050	1057	1069	1064	1052	1057
A_g	1054	1062	1038	1057	1052	1058	1049	1057	1053	1060	1049	1057
B_u	1035	1048	1034		1040	1050	1035	1057	1037	1047	1042	1057
A_g	1004	1013	1009	1008	1017	1028	1032		1018	1028	1033	
B_g	993	992	986	982	993	1002	990		978	983	976	982
B_u	945	954	939		934	940	956	948	969	977	970	982
A_u	923	932	962		918	923	917	932	915	924	935	932
B_g	905	914	926	927	888	897	904	897	891	893	906	897
A_g	883	882	885	882	867	875	875	882	883	886	888	882
A_u	863	871	880		862	871	865	873	863	871	877	873
B_g	854	862	869	854	838	847	851	842	847	857	860	854
B_u	831	839	837		828	835	837	824	829	837	844	824
A_g	826	833	847	824	737	738	726	728	812	818	818	
A_u	599	600	605		701	700	706	711	587	590	605	
B_u	428	427	457		444	443	469	456	421	422	441	438
A_g	363	364	376	376	343	342	346		378	377	393	394
A_g	287	284	304		310	308	329	307	319	317	328	329
A_u	188	184	190		232	229	255	239	196	196	212	
B_g	167	164	159		184	181	168		176	175	171	
B_u	127	124	134		158	150	144		132	130	125	
B_g	104	105	129		98	103	95		90	96	120	
A_u	83	79	101		76	78	82		73	71	87	
A_u	60	60	70		50	61	74		50	57	77	

[a] Wavenumbers higher than 1300 cm^{-1} are not given in this table. [b] Symmetry species of the normal vibrations for a point group C_{2h} molecule. [c] The 6-31G* basis set was used in the calculation. The calculated wavenumbers have been scaled by 0.95 for MP2 and 0.97 for B3LYP. [d] Calculated by using empirical force constants.[30] [e] Raman spectroscopy in the liquid state.[30] [f] Calculated in the present work.

(c) TGG and GGG Conformers. According to the preceding discussions, the TGG′ conformer is more dominant than the TGG conformer in the liquid and gaseous states. Recent molecular dynamics simulations of DME using an atomistic force field have indicated that, on going from the neat liquid to an aqueous solution of mole fraction 0.18, the population of the TGG conformer increases from 8% to 12%, while the population of the TGG′ conformer decreases from 17% to 9%.[53] A comparison of the calculated wavenumbers for the TGG and TGG′ conformers of the normal species shows that, although the wavenumbers are generally similar for the two conformers, distinctive wavenumber differences are noted in the 600−500 cm^{-1} region. Namely, the wavenumbers calculated by the MP2 method for the TGG and TGG′ conformers are 560 and 528 cm^{-1}, respectively, and those calculated by the B3LYP method are 537 and 527 cm^{-1}, respectively. Accordingly, we have carefully examined the Raman spectra of aqueous solutions of the normal species of DME and found that a shoulder band at about 555 cm^{-1}, which is ill-defined in the neat liquid, becomes stronger with increasing water fraction with respect to the 540 cm^{-1} band associated with the TGG′ conformer.[54] The band at about 555 cm^{-1} is therefore assigned to the TGG conformer with its wavenumber in agreement with the calculated results. The observation of this Raman band in the neat liquid, although it is not well-defined, is evidence for the presence of the TGG conformer in this state.

A close examination of the Raman spectrum of the perdeuterated species in the liquid state[30] indicates that a weak band at 1201 cm^{-1} is assigned to none of the TGT, TTT, TGG′, TTG, and TGG conformers, but is assigned reasonably to the GGG conformer, because the calculated wavenumber for this band is 1209 cm^{-1} by the MP2 method and is 1194 cm^{-1} by the B3LYP method. The presence of the GGG conformer in the liquid state is consistent with the results of the ab initio calculations showing that this conformer is the fifth most stable conformer of DME following TTG (Table 1).[24]

Force Constants. The force constants in the Cartesian coordinate space obtained by the MO and DFT calculations were transformed into those expressed in terms of the group symmetry coordinates.[4] In Table 7, the force constants thus obtained for the TGT conformer by the MP2 and B3LYP methods are listed in comparison with the corresponding empirical force constants[5,30] determined from the observed Raman and infrared wavenumbers. The listed values of the theoretical force constants have been scaled by $(0.95)^2$ and $(0.97)^2$, respectively, for the MP2 and B3LYP calculations, and only the force constants whose absolute values are larger than 0.03 in the pertinent units are given in Table 7.

The force constants of DME can be classified into the intragroup force constants and the intergroup force constants.[4] In the empirical force field for DME,[5,30] the second- and further-neighbor intergroup force constants were not considered except for the second-neighbor O−C stretching/C−C stretching force constant. The results in Table 7 indicate that the theoretical force constants calculated by the MP2 and B3LYP methods are very close to each other and are in good agreement in general

TABLE 7: Force Constants[a] for the TGT Conformer of 1,2-Dimethoxyethane

coordinate[b]	MP2[c]	B3LYP[d]	empirical[e]	coordinate[b]	MP2[c]	B3LYP[d]	empirical[e]
Intragroup $\underline{\mathrm{CH_3}}\mathrm{(O)}$							
CH_3 sym str (diagonal)	4.951	4.941	4.575	CH_3 sym str/sym def	0.106	0.101	
CH_3 sym def (diagonal)	0.658	0.660	0.679	CH_3 sym str/asym str (ip)	0.144	0.164	
CH_3 asym str (ip) (diagonal)	4.972	4.909	4.746	CH_3 asym str (ip)/asym def (ip)	−0.158	−0.163	
CH_3 asym def (ip) (diagonal)	0.590	0.592	0.570	CH_3 asym str (ip)/rock (ip)	0.070	0.080	
CH_3 rock (ip) (diagonal)	0.839	0.859	0.875	CH_3 asym def (ip)/rock (ip)	−0.066	−0.063	−0.022
CH_3 asym str (op) (diagonal)	4.731	4.635	4.746	CH_3 asym str (op)/asym def (op)	−0.149	−0.155	
CH_3 asym def (ip) (diagonal)	0.573	0.575	0.550	CH_3 asym str (op)/rock (op)	0.054	0.063	
CH_3 rock (op) (diagonal)	0.810	0.825	0.875	CH_3 asym def (op)/rock (op)	−0.039	−0.038	−0.022
Intragroup $\mathrm{(CH_3)}\underline{\mathrm{O}}\,\mathrm{(CH_2)}$							
COC bend (diagonal)	1.089	1.067	1.180				
Intragroup $\mathrm{(O)}\underline{\mathrm{CH_2}}\mathrm{(CH_2)}$							
CH_2 sym str (diagonal)	4.722	4.722	4.580	CH_2 sym str/scis	0.126	0.124	
CH_2 scis (diagonal)	0.597	0.601	0.581	CH_2 sym str/antisym str	−0.047	−0.042	
CH_2 antisym str (diagonal)	4.634	4.581	4.672	CH_2 sym str/OCC def	−0.096	−0.097	
CH_2 rock (diagonal)	0.834	0.851	0.896	CH_2 antisym str/rock	0.144	0.154	
CH_2 wag (diagonal)	0.737	0.750	0.753	CH_2 antisym str/twist	0.055	0.056	
CH_2 twist (diagonal)	0.672	0.680	0.693	CH_2 rock/twist	−0.098	−0.102	−0.118
OCC def (diagonal)	1.235	1.237	1.133	CH_2 wag/OCC def	0.066	0.070	0.128
Intergroup $\underline{\mathrm{CH_3{-}O}}\mathrm{(CH_2)}$ (First Neighbor)							
CH_3−O str (diagonal)	5.169	5.274	5.145	CH_3 sym def/CH_3−O str	−0.514	−0.521	−0.563
CH_3−O tor (diagonal)	0.077	0.079	0.066	CH_3 asym str (ip)/CH_3−O str	−0.083	−0.092	
CH_3−O str/COC bend	0.371	0.364	0.363	CH_3 asym str (ip)/COC bend	0.047	0.044	
CH_3 sym str/CH_3−O str	0.350	0.429		CH_3 rock (ip)/COC bend	0.091	0.097	0.012
Intergroup $\mathrm{(CH_3)}\underline{\mathrm{O{-}CH_2}}\mathrm{(CH_2)}$ (First Neighbor)							
O−C str (diagonal)	5.137	5.147	5.037	O−C str/CH_2 wag	−0.441	−0.448	−0.588
O−C tor (diagonal)	0.063	0.060	0.098	O−C str/OCC def	0.297	0.290	0.386
O−C str/CH_2 sym str	0.330	0.395		COC bend/O−C str	0.370	0.364	0.363
O−C str/CH_2 scis	−0.198	−0.200	−0.176	COC bend/OCC def	0.128	0.128	0.078
Intergroup $\mathrm{(O)}\underline{\mathrm{CH_2{-}CH_2}}\mathrm{(O)}$ (First Neighbor)							
C−C str (diagonal)	4.565	4.351	4.240	CH_2 rock/CH_2 twist	0.041	0.042	0.029
C−C tor (diagonal)	0.135	0.125	0.123	CH_2 rock/CCO def	0.105	0.114	0.016
CH_2 sym str/C−C str	0.071	0.089		CH_2 wag/C−C str	0.208	0.211	0.221
CH_2 scis/C−C str	−0.109	−0.108	−0.102	CH_2 wag/CH_2 twist	−0.034	−0.033	−0.026
CH_2 antisym str/CCO def	0.085	0.084		CH_2 wag/CCO def	0.038	0.034	−0.010
CH_2 rock/C−C tor	−0.050	−0.045		CH_2 twist/CCO def	0.134	0.136	0.072
CH_2 rock/CH_2 rock	0.048	0.042	−0.050	OCC def/C−C str	0.225	0.223	0.037
CH_2 rock/CH_2 wag	−0.038	−0.037	−0.063	OCC def/CCO def	−0.080	−0.085	0.146
Intergroup $\underline{\mathrm{CH_3{-}}}\mathrm{(O)}\underline{\mathrm{{-}CH_2}}\mathrm{(CH_2)}$ (Second Neighbor)							
CH_3 sym str/O−C str	−0.023	−0.033		CH_3−O str/CH_2 wag	0.111	0.118	
CH_3 sym def/O−C str	0.059	0.064		CH_3−O str/OCC def	0.133	0.130	
CH_3 rock (ip)/O−C str	0.135	0.140					
Intergroup $\mathrm{(CH_3)}\underline{\mathrm{O{-}}}\mathrm{(CH_2)}\underline{\mathrm{{-}CH_2}}\mathrm{(O)}$ (Second Neighbor)							
O−C str/C−C str	0.241	0.286	0.314	O−C str/CH_2 twist	0.040	0.039	
O−C str/C−C tor	−0.048	−0.045		O−C str/CCO def	−0.048	−0.045	
O−C str/CH_2 rock	0.079	0.081		COC bend/C−C str	0.056	0.053	
O−C str/CH_2 wag	0.028	0.031					
Intergroup $\mathrm{(CH_3)}\underline{\mathrm{O{-}}}\mathrm{(CH_2CH_2)}\underline{\mathrm{{-}O}}\mathrm{(CH_3)}$ (Third Neighbor)							
O−C str/C−O str	0.024	0.036					

[a] Only the force constants whose absolute values are larger than 0.03 in the pertinent units are given in this table. Units are mdyn Å^{-1} for the diagonal stretching and off-diagonal stretching−stretching force constants, mdyn for the off-diagonal stretching−bending and stretching−torsion force constants, and mdyn Å for the diagonal bending and torsion and off-diagonal bending−bending and bending−torsion force constants. [b] The group symmetry coordinates were defined by the conventions recommended by IUPAC.[4,55] In defining the coordinates of the methyl and methylene groups for the MP2 and B3LYP force constants, the valence angles were assumed to be tetrahedral and the corresponding coordinates for the two methyl or methylene groups are symmetrical with respect to the 2-fold axis in the molecule. Key: sym, symmetric; asym, asymmetric; antisym, antisymmetric; scis, scissor; def, deformation; str, stretch; tor, torsion; ip, in-plane; op, out-of-plane. O−C and C−O imply O−CH_2 and CH_2−O, respectively. [c] The force constants have been scaled by $(0.95)^2$. [d] The force constants have been scaled by $(0.97)^2$. [e] Taken from ref 30.

with the empirical force constants. The consistency of these sets of force constants proves the validity of their values and accordingly the validity of the wavenumbers and assignments calculated therefrom.

In the theoretical force field obtained in this work, the intragroup and first-neighbor intergroup off-diagonal force constants between the C−H stretching (CH_3 symmetric and asymmetric stretching and CH_2 symmetric and antisymmetric stretching) and other coordinates are important, although these force constants were assumed to be zero in the empirical force field because of their indeterminacy from the experimental data. The theoretical results also show that the off-diagonal force constants associated with the skeletal stretching (O−C and C−C stretching) as one of the relevant coordinates are significant even between the second- or third-neighbor groups. These force constants were again assumed to be zero in the empirical force field.

Conclusions

The conformations and vibrations of DME have been studied by various DFT and MO methods. The energies of conformers were better predicted by the DFT methods using the B3 exchange functional than other methods. The vibrational wavenumbers calculated by the DFT and MO methods explained, after correcting with uniform scaling, the observed Raman and infrared spectra of the normal and perdeuterated species of DME. It was confirmed that the conformer of DME present in the solid state is TGT, and the conformers in the liquid state are TGT, TTT, TGG′, and TTG. The present calculations further indicated that the TGG and GGG conformers are also present in the liquid state. The distributions of the ratio of the unscaled calculated wavenumber to the experimental wavenumber, $\nu_{\mathrm{calc}}/\nu_{\mathrm{exp}}$, are narrower with the B3PW91 and B3LYP methods than with other methods, indicating that these two methods, when making appropriate uniform scaling corrections, give wavenumbers in excellent agreement with the experimental wavenumbers. In conclusion, the performance of the B3PW91 and B3LYP methods is the best among the DFT and MO methods used in this work in reproducing the experimental results of the energies, molecular geometries, and vibrational wavenumbers for DME.

References and Notes

(1) Wilson, E. B., Jr. *J. Chem. Phys.* **1939**, *7*, 1047.

(2) Shimanouchi, T. In *Physical Chemistry: An Advanced Treatise*; Eyring, H., Henderson, D., Jost, W., Eds.; Academic Press: New York, 1970; Vol. IV, pp 233−306.

(3) Califano, S. *Vibrational States*; Wiley: London, 1976; pp 207−265.

(4) Matsuura, H.; Tasumi, M. In *Vibrational Spectra and Structure*; Durig, J. R., Ed.; Elsevier: Amsterdam, 1983; Vol. 12, pp 69−143.

(5) Shimanouchi, T.; Matsuura, H.; Ogawa, Y.; Harada, I. *J. Phys. Chem. Ref. Data* **1978**, *7*, 1323.

(6) Shimanouchi, T.; Matsuura, H.; Ogawa, Y.; Harada, I. *J. Phys. Chem. Ref. Data* **1980**, *9*, 1149.

(7) Pulay, P. *Mol. Phys.* **1971**, *21*, 329.

(8) Schlegel, H. B.; Wolfe, S.; Bernardi, F. *J. Chem. Phys.* **1975**, *63*, 3632.

(9) Blom, C. E.; Altona, C. *Mol. Phys.* **1976**, *31*, 1377.

(10) The term “frequency” has been customarily used in the field of vibrational spectroscopy to indicate the quantity actually given in units of cm^{-1} rather than Hz. We use, in this paper, the appropriate terminology of “wavenumber” for this quantity, following SI usage recommended by IUPAC.[11]

(11) Mills, I.; Cvitaš, T.; Homann, K.; Kallay, N.; Kuchitsu, K. *Quantities, Units and Symbols in Physical Chemistry*; IUPAC, Blackwell: Oxford, 1988.

(12) Pulay, P.; Fogarasi, G.; Pongor, G.; Boggs, J. E.; Vargha, A. *J. Am. Chem. Soc.* **1983**, *105*, 7037.

(13) Fogarasi, G.; Pulay, P. *Annu. Rev. Phys. Chem.* **1984**, *35*, 191.

(14) Parr, R. G.; Yang, W. *Density-Functional Theory of Atoms and Molecules*; Oxford University Press: New York, 1989.

(15) Johnson, B. G.; Gill, P. M. W.; Pople, J. A. *J. Chem. Phys.* **1993**, *98*, 5612.

(16) Becke, A. D. *J. Chem. Phys.* **1993**, *98*, 5648.

(17) Rauhut, G.; Pulay, P. *J. Phys. Chem.* **1995**, *99*, 3093.

(18) El-Azhary, A. A.; Suter, H. U. *J. Phys. Chem.* **1996**, *100*, 15056.

(19) Scott, A. P.; Radom, L. *J. Phys. Chem.* **1996**, *100*, 16502.

(20) Yoshida, H.; Harada, T.; Matsuura, H. *J. Mol. Struct.* **1997**, *413/414*, 217.

(21) Barzaghi, M.; Gamba, A.; Morosi, G. *J. Mol. Struct.* (*THEOCHEM*) **1988**, *170*, 69.

(22) Yoshida, H.; Kaneko, I.; Matsuura, H.; Ogawa, Y.; Tasumi, M. *Chem. Phys. Lett.* **1992**, *196*, 601.

(23) Murcko, M. A.; DiPaola, R. A. *J. Am. Chem. Soc.* **1992**, *114*, 10010.

(24) Tsuzuki, S.; Uchimaru, T.; Tanabe, K.; Hirano, T. *J. Phys. Chem.* **1993**, *97*, 1346.

(25) Jaffe, R. L.; Smith, G. D.; Yoon, D. Y. *J. Phys. Chem.* **1993**, *97*, 12745.

(26) Ogawa, Y.; Ohta, M.; Sakakibara, M.; Matsuura, H.; Harada, I.; Shimanouchi, T. *Bull. Chem. Soc. Jpn.* **1977**, *50*, 650.

(27) Astrup, E. E. *Acta Chem. Scand., Ser. A* **1979**, *33*, 655.

(28) Inomata, K.; Abe, A. *J. Phys. Chem.* **1992**, *96*, 7934.

(29) Yoshida, H.; Tanaka, T.; Matsuura, H. *Chem. Lett.* **1996**, 637.

(30) Matsuura, H.; Fukuhara, K.; Tamaoki, H. *J. Mol. Struct.* **1987**, *156*, 293.

(31) Flory, P. J. *Statistical Mechanics of Chain Molecules*; Hanser: Munich, 1989; pp 165−172.

(32) Andersson, M.; Karlström, G. *J. Phys. Chem.* **1985**, *89*, 4957.

(33) Becke, A. D. *Phys. Rev. A* **1988**, *38*, 3098.

(34) Vosko, S. H.; Wilk, L.; Nussair, M. *Can. J. Phys.* **1980**, *58*, 1200.

(35) Perdew, J. P. *Phys. Rev. B* **1986**, *33*, 8822; **1986**, *34*, 7406.

(36) Lee, C.; Yang, W.; Parr, R. G. *Phys. Rev. B* **1988**, *37*, 785.

(37) Perdew, J. P. In *Electronic Structure of Solids ’91*; Ziesche, P., Eschrig, H., Eds.; Akademie Verlag: Berlin, 1991.

(38) Perdew, J. P.; Wang, Y. *Phys. Rev. B* **1992**, *45*, 13244.

(39) Perdew, J. P.; Chevary, J. A.; Vosko, S. H.; Jackson, K. A.; Pederson, M. R.; Singh, D. J.; Fiolhais, C. *Phys. Rev. B* **1992**, *46*, 6671.

(40) Frisch, M. J.; Trucks, G. W.; Schlegel, H. B.; Gill, P. M. W.; Johnson, B. G.; Robb, M. A.; Cheeseman, J. R.; Keith, T.; Petersson, G. A.; Montgomery, J. A.; Raghavachari, K.; Al-Laham, M. A.; Zakrzewski, V. G.; Ortiz, J. V.; Foresman, J. B.; Cioslowski, J.; Stefanov, B. B.; Nanayakkara, A.; Challacombe, M.; Peng, C. Y.; Ayala, P. Y.; Chen, W.; Wong, M. W.; Andres, J. L.; Replogle, E. S.; Gomperts, R.; Martin, R. L.; Fox, D. J.; Binkley, J. S.; Defrees, D. J.; Baker, J.; Stewart, J. P.; Head-Gordon, M.; Gonzalez, C.; Pople, J. A. *GAUSSIAN 94*, Revision D.3; Gaussian Inc.: Pittsburgh, PA, 1995.

(41) Shimanouchi, T. *Computer Programs for Normal Coordinate Treatment of Polyatomic Molecules*; The University of Tokyo, 1968.

(42) Yoshida, H.; Tasumi, M. *J. Chem. Phys.* **1988**, *89*, 2803.

(43) Yokoyama, Y.; Uekusa, H.; Ohashi, Y. *Chem. Lett.* **1996**, 443.

(44) Machida, K.; Miyazawa, T. *Spectrochim. Acta* **1964**, *20*, 1865.

(45) Snyder, R. G.; Zerbi, G. *Spectrochim. Acta, Part A* **1967**, *23*, 391.

(46) Iwamoto, R. *Spectrochim. Acta, Part A* **1971**, *27*, 2385.

(47) Matsuura, H.; Miyazawa, T.; Machida, K. *Spectrochim. Acta, Part A* **1973**, *29*, 771.

(48) Matsuura, H.; Fukuhara, K. *J. Mol. Struct.* **1985**, *126*, 251.

(49) Matsuura, H.; Fukuhara, K. *J. Polym. Sci., Part B: Polym. Phys.* **1986**, *24*, 1383.

(50) Begum, R.; Matsuura, H. *J. Chem. Soc., Faraday Trans.* **1997**, *93*, 3839.

(51) Matsuura, H.; Fukuhara, K.; Tamaoki, H. *J. Sci. Hiroshima Univ., Ser. A* **1985**, *49*, 89.

(52) Smith, G. D.; Jaffe, R. L.; Yoon, D. Y. *J. Am. Chem. Soc.* **1995**, *117*, 530.

(53) Bedrov, D.; Pekny, M.; Smith, G. D. *J. Phys. Chem. B* **1998**, *102*, 996.

(54) Matsuura, H. Unpublished results.

(55) IUPAC Commission on Molecular Structure and Spectroscopy. *Pure Appl. Chem.* **1978**, *50*, 1707.